Available online at www.sciencedirect.com
SCIENCE DIRECT
Catalysis Today 114 (2006) 211–216
CATALYSIS TODAY
www.elsevier.com/locate/cattod

Catalytic properties of dealuminated ferrierite type zeolite studied in transformations of *m*-xylene Part 2

R. Rachwalik [a], Z. Olejniczak [b], B. Sulikowski [a,*]

[a] *Institute of Catalysis and Surface Chemistry, Polish Academy of Sciences, Niezapominajek 8, 30–239 Kraków, Poland*
[b] *Institute of Nuclear Physics, Polish Academy of Sciences, Radzikowskiego 152, 31–342 Kraków, Poland*

Available online 9 March 2006

Abstract

The ammonium form of ferrierite (obtained from K,Na-ferrierite, Tosoh) was modified with aqueous solution of hydrochloric acid of different concentration. It has been demonstrated that ferrierite is amenable to HCl solution treatment, while retaining its high crystallinity (XRD, SEM). Dealumination proceeded smoothly and 60% of aluminium was easily removed from the sample just upon 0.25 M HCl treatment. ^{29}Si NMR revealed that during the acid treatment the aluminium atoms were removed preferentially from Si(2Al) and Si(1Al) T_B positions. Acidity of the samples was assessed by sorption of CO and ammonia and using FT IR spectroscopy. Studies of *m*-xylene transformations showed increased activity of the samples with increasing level of dealumination. Such behaviour was attributed to a particular morphology of the parent ferrierite. Dealumination of zeolite with the plate-like morphology yields a highly active material, coupled with high *para*-selectivity after the first acid treatment.

Keywords: Ferrierite (Tosoh); Dealumination; ^{27}Al MAS NMR; ^{29}Si MAS NMR; CO and NH_3 sorption; *m*-Xylene transformations

1. Introduction

The framework Si/Al molar ratio of zeolites belongs to important parameters exerting a strong influence on numerous properties, such as the concentration and strength of Brønsted acid sites, thermal and hydrothermal stability, hydrophobicity, sorption, catalytic activity and selectivity [1]. The Si/Al framework ratio can be controlled either during the hydrothermal synthesis of zeolites, or during various post-synthesis modifications obeying dealumination and realumination [2]. Dealumination is defined as a partial or total removal of aluminium from zeolite frameworks by thermal treatment or chemical reactions. The processes that allow to remove aluminium from the tetrahedral sites can be divided into the two groups: (i) those proceeding without any external source of silicon (carried out either by hydrothermal treatments, or by chemical reactions with mineral acids and chelating agents) and (ii) those requiring an additional external source of silicon, exemplified by molecules like $SiCl_4$ [3,4] or $(NH_4)_2SiF_6$, used in the gas or liquid phase, respectively.

Since the number of Brønsted acid sites in zeolites controlling their catalytic activity is inadvertently linked to the number of aluminium atoms occupying tetrahedral positions, a large effort was devoted to the manipulation of the Si/Al ratio. There are zeolites which can be synthesised directly with a limited Si/Al framework ratio (e.g. X and Y zeolites), while others can be prepared in a broad range of framework aluminium ending with a pure silica counterpart (Silicalite-I of ZSM-5 family). Various dealumination methods are known. Dealumination with $SiCl_4$ and $(NH_4)_2SiF_6$ is well documented [5,6]. Aluminium can also be removed from tetrahedral positions by a number of other agents, like $COCl_2$, CCl_4, SO_2Cl_2 and also by organic and inorganic acids (H_4EDTA, tartaric acid, diethylenotriaminopentaacetic acid, HNO_3 and HCl) [2]. Moreover, even if zeolite can be prepared with the same number of aluminium per unit cell, by direct synthesis or by post-synthesis dealumination, the properties of two solids will be different. In general, dealumination of

* Corresponding author. Tel.: +48 12 3695 127; fax: +48 12 425 1923.
E-mail address: ncsuliko@cyf-kr.edu.pl (B. Sulikowski).

0920-5861/$ – see front matter © 2006 Elsevier B.V. All rights reserved.
doi:10.1016/j.cattod.2006.01.021

crystalline aluminosilicates often leads to imperfect zeolitic frameworks, due to the formation of both framework defects ('hydroxyl nests') and secondary mesoporosity [7]. Such crystals exhibit catalytic activity dissimilar from those obtained by a direct synthesis. On the other hand, the use of simple dealumination method is desirable for practical applications. Hence, we have studied physicochemical and catalytic properties of a series of solids prepared by the acid treatment of ferrierite.

Ferrierite has been classified in the group no. 6 by Breck [8], and its structure has been solved by Vaughan [9] and Kerr [10]. The unit cell of ferrierite is composed of 36 T atoms (where T = Si, Al) and Si/Al ratios are generally in the range 3.2–6.2, corresponding to 5–8.6 Al per unit cell. Ferrierite is quite distinct from most known zeolites as the four-membered rings are the smallest ones building its framework.

Transformations of alkylaromatic hydrocarbons were used to monitor the behaviour of acid centres in zeolites of different structure, but only few papers considered the ferrierite type zeolite [11,12]. Still, it is an important catalyst that is produced commercially and applied in isomerization of butenes on the industrial scale.

In the previous work the dealumination of a ferrierite manufactured by Zeolyst was described [12, Part 1], while in the present paper properties of ferrierite produced by Tosoh were studied. The parent K,Na-ferrierite form was transformed into the ammonium form, which was subjected to the hydrochloric acid treatment of different concentration. The parent and dealuminated ferrierite samples were then studied in *m*-xylene transformations using a continuous-flow microreactor.

2. Experimental

The K–Na form of ferrierite with the Si to Al molar ratio of 9.2 (Tosoh, Japan) was four-fold ion-exchanged by using 0.5 M ammonium nitrate solution. The ammonium form was treated with aqueous hydrochloric acid solutions of various concentration. First, the NH_4-FER was treated with 0.25 M HCl at ambient temperature for 4 h. During dealumination, the amount of the acid solution was kept at 30 cm^3 for 1 g of the zeolite. After the treatment, the sample was thoroughly washed with distilled water, dried at 353 K overnight and calcined in air at 773 K for 5 h to yield the catalyst labelled FE1 (0.25 HCl). This FE1 (0.25 HCl) sample was then subjected to a similar procedure, using 1 M HCl (cf. Fig. 1), and the sample obtained was denoted FE2 (1.0 HCl). Finally, the sample FE3 (2.0 HCl) was obtained from FE2 (1.0 HCl), by applying treatment with 2 M HCl.

Powder X-ray diffraction (XRD) patterns for 2θ ranging from 5 to 50° were measured on a Siemens D5005 automatic diffractometer with Cu Kα radiation. The SEM pictures were taken with a Philips XL30 instrument.

Solid-state magic-angle-spinning nuclear magnetic resonance (MAS NMR) spectra were measured on a home-made pulse NMR spectrometer at the magnetic field of 7.05 T. A Bruker HP-WB high-speed MAS probe equipped with the 4 mm zirconia rotor and KEL-F cap was used to record the MAS spectra at the spinning speed ranging from 4 to 7 kHz. All the NMR spectra shown here were normalised, taking into account the number of acquisitions and the sample mass. The dealumination level of ferrierite was monitored quantitatively using ^{27}Al MAS NMR measurements.

FTIR experiments (for sorption of both ammonia and CO) were performed on the self-supported discs of zeolites (about 10 mg cm^{-2}) with a BRUKER 48 PC spectrometer equipped with an MCT detector. The spectral resolution was 2 cm^{-1}, and 100–200 scans were recorded. The ferrierite samples were activated in situ in the IR cell at 803 K for 2 h under a vacuum of 10^{-6} Pa.

The continuous-mode isomerization of *m*-xylene was performed using a tubular down-flow stainless steel microreactor (diameter 0.9 cm) with 500 mg of catalyst (0.250–0.315 mm fraction) and 2 cm^3 of SiC chips (>400 μm fraction). The catalyst was activated in helium flow at 753 K for 1 h. *m*-Xylene was fed by a syringe pump to obtain WHSV = 1.5 under the atmospheric pressure. The conversion and other parameters were calculated as shown below:

$$X_{m\mathrm{X}} = \left[\frac{98.62 - c_{m\mathrm{X}}}{98.62}\right] \times 100\%$$

$$\frac{S_\mathrm{I}}{S_\mathrm{D}} = \frac{(c_{p\mathrm{X}} - 0.93) + (c_{o\mathrm{X}} - 0.45)}{(c_{1,2,3\text{-TMB}} + c_{1,2,4\text{-TMB}} + c_{1,3,5\text{-TMB}}) \times 2}$$

$$\frac{p\text{-xylene}}{o\text{-xylene}} = \frac{c_{p\mathrm{X}} - 0.93}{c_{o\mathrm{X}} - 0.45}$$

$$S_{p\mathrm{X}} = \left[\frac{c_{p\mathrm{X}} - 0.93}{98.62 - c_{m\mathrm{X}}}\right] \times 100\%$$

where $X_{m\mathrm{X}}$ denotes the conversion of *m*-xylene (mol%), $S_\mathrm{I}/S_\mathrm{D}$ the ratio of the selectivity of *m*-xylene isomerization to the selectivity of *m*-xylene disproportionation, and $S_{p\mathrm{X}}$ the selectivity of *p*-xylene formation. The $c_{m\mathrm{X}}$, $c_{p\mathrm{X}}$, $c_{o\mathrm{X}}$, $c_{1,2,3\text{-TMB}}$, $c_{1,2,4\text{-TMB}}$, $c_{1,3,5\text{-TMB}}$ denote the concentrations (mol%) of *m*-, *p*-, *o*-xylene, 1,2,3-, 1,2,4- and 1,3,5-TMB in products, respectively.

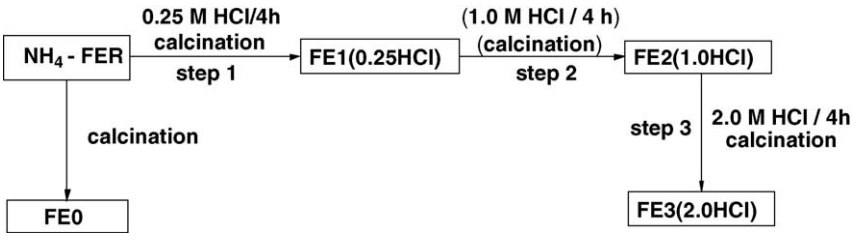

Fig. 1. A scheme showing preparation of the samples.

The corresponding concentrations of *m*-xylene, *p*-xylene and *o*-xylene in the feed were equal to 98.62, 0.93 and 0.45 mol%.

3. Results and discussion

The ammonium form of ferrierite was dealuminated with HCl acid of increasing concentration, according to the procedure shown in Fig. 1. The XRD diffraction patterns of the solids revealed that ferrierite after acid treatment preserved its structure and no other phases were detected (Fig. 2). Therefore, acid treatment did not affect the integrity of zeolite crystals. As observed before, dealumination produces samples with a small and anisotropic unit cell contraction [12].

In Fig. 3, scanning electron microscopy (SEM) microphotographs of the parent and highly dealuminated sample are compared. The NH_4-FER starting material consists of agglomerates of very small zeolite crystals. The crystals reveal plate-like morphology, with planar dimensions of about 0.5–1 μm, and very small thickness (<0.1 μm). After the last dealumination step the morphology of the sample FE3 essentially does not change. The highly crystalline according to X-rays sample exhibits a similar plate-like morphology. The crystals size and their thickness are not affected by the hydrochloric acid leaching (Fig. 3b).

The course of ferrierite dealumination was monitored quantitatively using ^{27}Al MAS NMR. In all the spectra visualized in Fig. 4 in the absolute mode, a well-developed signal at about 54 ppm is seen, while signals attributed to the octahedrally coordinated aluminium at ∼0 ppm were absent. The signals at 54 ppm are due to aluminium in tetrahedral coordination, and their intensity was followed quantitatively after consecutive treatments with hydrochloric acid. The results are plotted in Fig. 5. As seen, the dealumination of this ferrierite proceeds smoothly and efficiently, and aluminium is progressively removed from the tetrahedral sites. Already after the first treatment by diluted 0.25 M HCl, about 60 wt.% of aluminium was removed from the lattice positions. With the repetition of the procedure using 1 and 2 M HCl, further dealumination of ferrierite is observed, giving eventually a sample FE3 with 80% dealumination level.

^{29}Si MAS NMR was applied for quantitative measurements of the Si/Al framework ratio. The ^{29}Si MAS NMR spectrum of

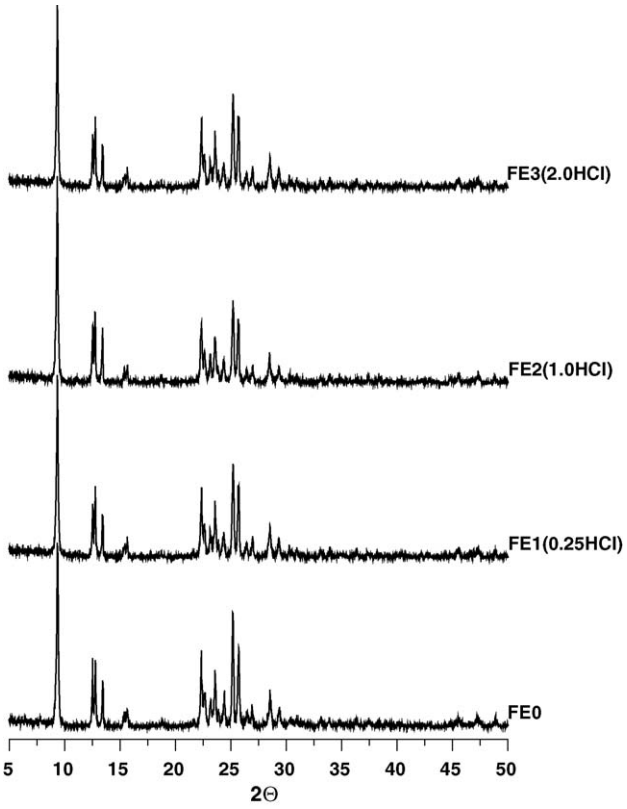

Fig. 2. X-ray diffraction patterns of the parent and dealuminated forms of ferrierite.

NH_4-ferrierite is a superposition of many signals. After Gaussian deconvolution four signals at −105, −109, −115.5 and −112 ppm were obtained and assigned to the Si(1Al) and Si(0Al) groupings located at T_A and T_B framework positions (Fig. 6a). The deconvoluted signals were denoted: Si(1Al) T_A, Si(1Al) T_B, Si(0Al) T_B and Si(0Al) T_A, respectively. Another signal at −99 ppm can be attributed either to the Si(2Al) or Si(OH) positions (Fig. 6b) [13]. The Si/Al ratio obtained for FE0 and FE3 (2.0 HCl) samples were 9.1 and 40.5, thus confirming the progress of dealumination observed by ^{27}Al NMR. As can be also seen in Fig. 6b, the aluminium atoms located at Si(2Al) and Si(1Al) T_B positions are eliminated preferentially during the acid treatment.

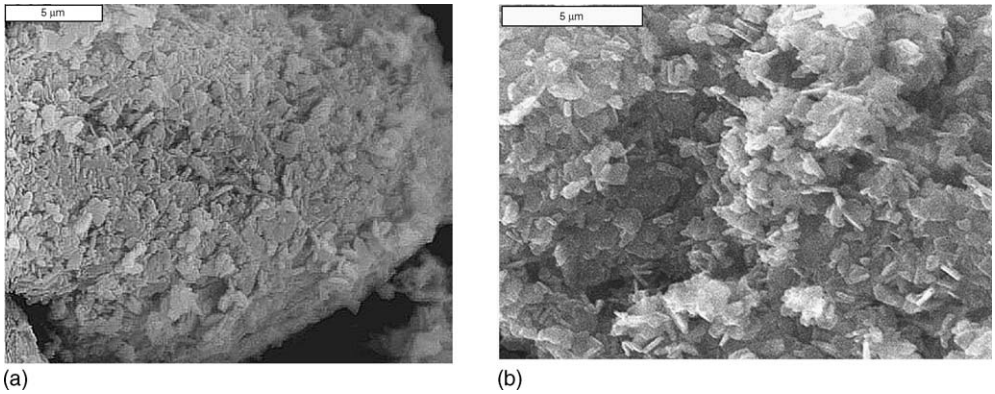

Fig. 3. Scanning electron microscopy microphotographs of: (a) starting material NH_4-FER, Si/Al = 9.2); and (b) dealuminated sample FE3 (Si/Al = 40.5).

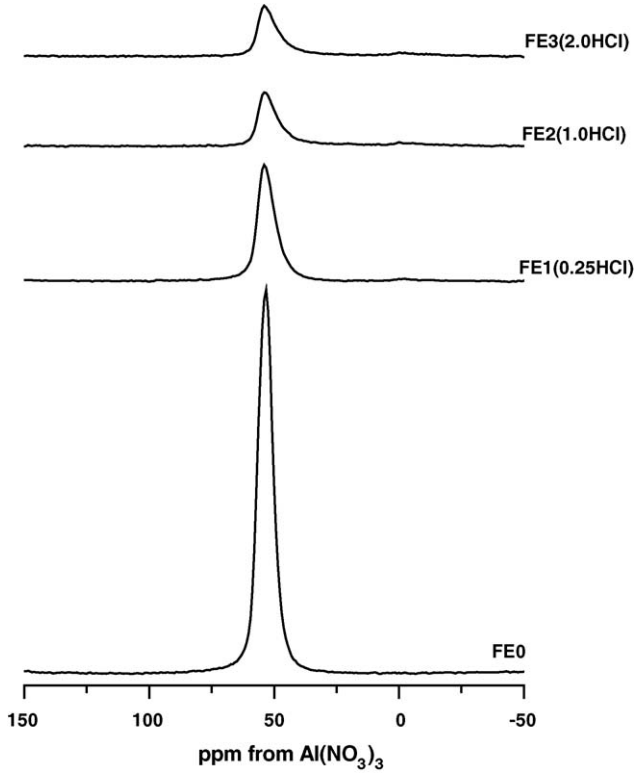

Fig. 4. ^{27}Al MAS NMR spectra of ferrierite samples.

For selected samples the FTIR measurements were carried out using sorption of ammonia and CO. By applying IR spectroscopy it was therefore possible to examine the interactions between the parent FEO and its deeply-dealuminated form. The evolution of the acid samples upon dealumination was followed, in terms of the nature of acid sites and their strength. As shown in Fig. 7, the FTIR spectrum of the FEO consists of five bands. The signal at 2172 cm^{-1} is attributed to CO adsorbed on the Brønsted acid sites, while the intensity of the band at 2190 cm^{-1} is assigned to CO interacting with Lewis acid sites (extraframework species). Additionally, the signals at 2230 and 2200 cm^{-1}, attributed to Lewis acid

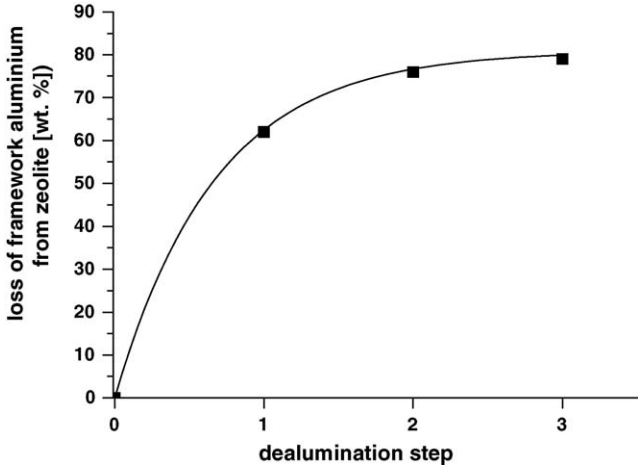

Fig. 5. Loss of aluminium from zeolite framework vs. dealumination step.

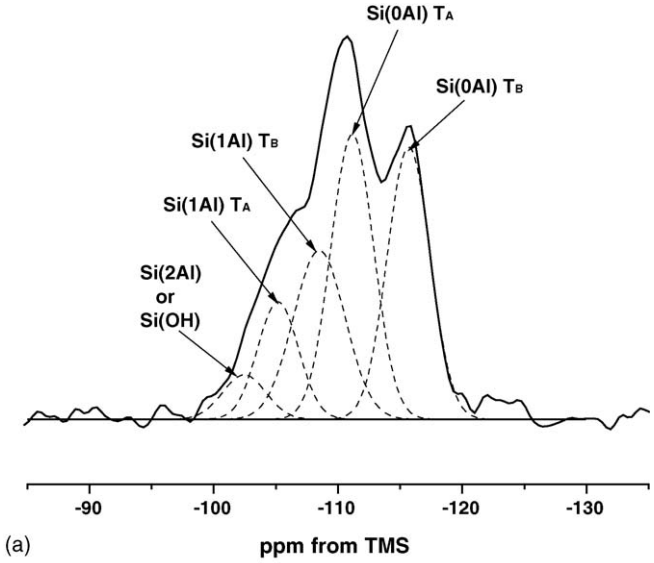

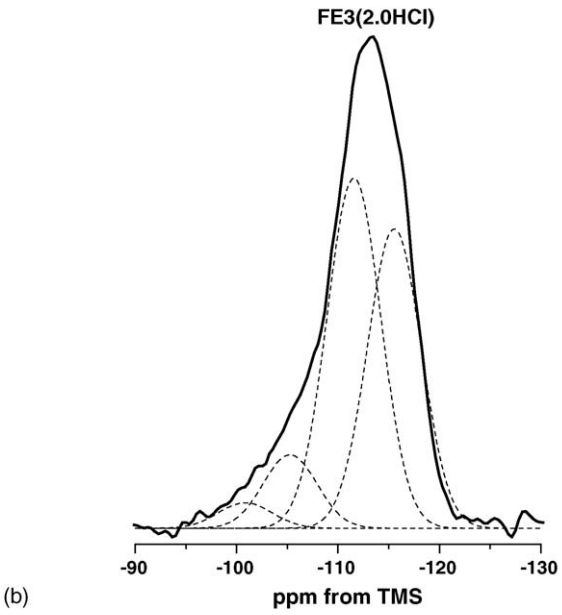

Fig. 6. ^{29}Si MAS NMR spectra of parent ferrierite NH_4-FER and its dealuminated form FE3(2.0HCl).

sites formed during zeolite dehydroxylation, can be discerned in the spectrum.

The IR bands of OH groups in the hydrogen form of ferrierite (FE0) and in the sample obtained after the third dealumination step [FE3(2.0HCl)] are compared in Fig. 8. In the parent material the band of Si–OH–Al groups is composed of a very strong signal at 3600 cm^{-1} accompanied by two much weaker shoulders at ~3550 and 3650 cm^{-1}. According to Datka et al. [14], the bands at 3600 and 3550 cm^{-1} are due to hydroxyl groups, located inside the 10-membered-ring channels and inside the ferrierite cages, respectively. As the dealumination is advanced (Fig. 8, trace b), a significant decrease of the main peak at 3600 cm^{-1} is observed, thus confirming depletion of aluminium from tetrahedral sites. Simultaneously, an increase of the shoulder intensity at

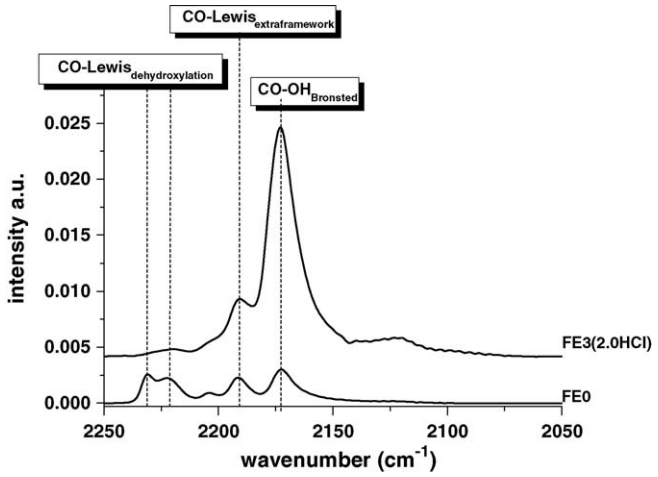

Fig. 7. FT IR spectra of ferrierite samples after adsorption of CO.

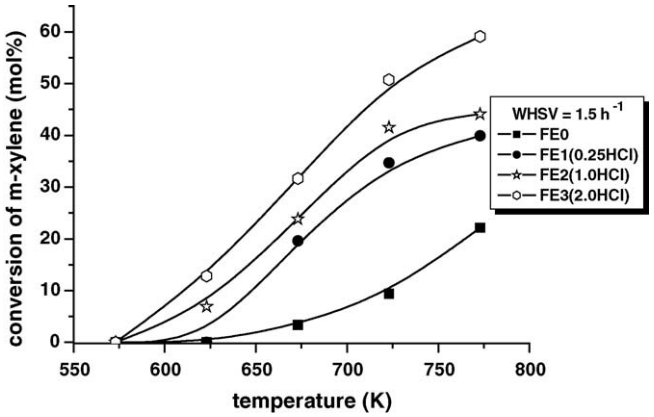

Fig. 9. Conversion of *m*-xylene (mol%) as a function of temperature for the isomerization of the parent FE0 and dealuminated catalysts.

3650 cm^{-1} can be noticed. Peixoto et al. claim that this additional band can be related to the extraframework aluminium species [15]. In our opinion, the signal at 3650 cm^{-1} should be attributed rather to framework defects formed upon aluminium depletion, because no signals of the extraframework aluminium were present in the ^{27}Al MAS NMR spectra, and very small amounts of these species were identified by IR spectroscopy.

Catalytic properties of the parent and dealuminated samples studied in a continuous-flow microreactor are summarized in Figs. 9 and 10. Upon HCl treatment progressively higher conversions in the series of dealuminated samples have been observed. The FE3 (2.0 HCl) material with 80% dealumination level was surprisingly the most active catalyst (Fig. 9). It is therefore clear that the modification of the ferrierite of Tosoh exerts strong and positive effect on the rate of *m*-xylene transformation.

In Fig. 10, the change of the course of *m*-xylene transformation is shown against the number of acid treatments. Both the starting material and the sample obtained after the first step give the same isomerisation to disproportionation ratio of 9, and upon further treatments the S_I/S_D index decreases considerably to 2 (Fig. 10b). In other words, the two samples, parent and FE1 (0.25 HCl), have strong preponderance of isomerization over disproportionation reaction path. Interestingly, even the FE1 (0.25 HCl) sample, although generally more active than FE0, is still very selective. The shift of the *m*-xylene transformation towards the disproportionation route became significant after the second and third leaching with HCl (Fig. 10b).

The shape-selectivity of isomerization, expressed as *p*-xylene to *o*-xylene ratio in the products, is also high, and ranges from 3 to 4 for the FE0 and FE1 (0.25 HCl) samples (Fig. 10a). This ratio decreases dramatically for the sample obtained after the third dealumination step and becomes close to thermodynamic equilibrium. The overall selectivity to *p*-xylene is visualized in Fig. 10c. It is within 60–65% for the two samples

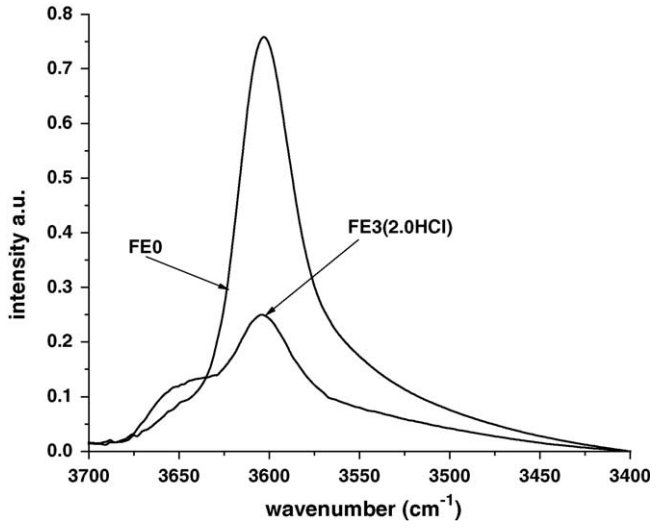

Fig. 8. FT IR spectra of OH groups in FE0 and dealuminated sample FE3(2.0HCl).

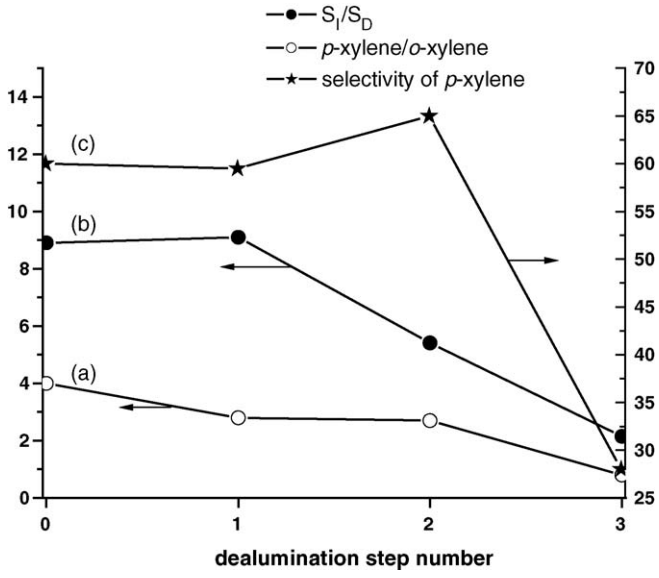

Fig. 10. Parameters of *m*-xylene transformation: (a) *p*-xylene/*o*-xylene molar ratio; (b) selectivity of *m*-xylene isomerization to selectivity of *m*-xylene disproportionation (S_I/S_D); and (c) selectivity of *p*-xylene formation (%) as a function of dealumination steps.

FE0 and FE1 (0.25 HCl), and lowers to only 30% for the highest dealuminated sample FE3 (2.0 HCl). The product obtained over this sample is very rich in *p*-xylene (about 90 mol%), while the concentration of the *para*-isomer at thermodynamic equilibrium is only 24.4 mol% [16].

Different behaviour of the two synthetic ferrierite samples upon mineral acid treatment, i.e. Zeolyst, described earlier [12] and Tosoh, may be attributed tentatively to dissimilar morphology of the starting materials. The Zeolyst sample consists of regular crystals 0.5–2 μm (not shown), while the Tosoh sample has plate-like morphology (Fig. 3), which enables better access of hydrochloric acid during the treatment. Hence, much higher dealumination levels can be obtained using the latter sample. When the dealumination level is advanced, formation of a secondary mesoporous system is observed in the samples. Thus, more and more Brønsted acid centres are becoming available for the substrate. As these sites are now less confined geometrically due to the presence of mesopores, the ratio between the *p*- and *o*-xylene in the products is approaching one, i.e. the value that is typical for thermodynamic equilibrium of C_8 aromatic hydrocarbons [16].

4. Conclusions

Treatment of synthetic ferrierite by hydrochloric acid is an efficient way of catalyst modification. The final result depends strongly on the type of parent zeolite used. Under the same experimental conditions, as demonstrated here and in the previous paper [12], very different solids can be obtained. While 18% dealumination level was observed after 0.25 M HCl treatment of ferrierite from Zeolyst, 60% was found starting from the Tosoh material. It was observed that aluminium atoms located at Si(2Al) and Si(1Al) T_B positions are eliminated preferentially during the acid treatment. Dealumination of zeolite with the plate-like morphology yields highly active materials, with high *para*-selectivity maintained after the first acid treatment.

Fine-tuning of the zeolitic catalysts becomes now possible by choosing a proper parent material with the same structure. Moreover, reactions of larger than xylenes molecules will now become feasible on this medium-pore zeolite [17], due to development of mesopores upon modification.

Acknowledgements

We are grateful to the EU for the Marie Curie Action grant *TOK-CATA* (no. MTKD-CT-2004-509832). We are also indebted to Professor Jerzy Datka of the Jagiellonian University, Kraków, for IR measurements.

References

[1] J. Scherzer, ACS Symp. Ser. 248 (1984) 157.
[2] H. Hamdan, B. Sulikowski, J. Klinowski, J. Phys. Chem. 93 (1989) 350; B. Sulikowski, Heterogen. Chem. Rev. 3 (1996) 203.
[3] H.K. Beyer, I.M. Belenykaja, in: B. Imelik, et al. (Eds.), Catalysis by Zeolites, Elsevier, Amsterdam, 1980, p. 203.
[4] B. Sulikowski, G. Borbély, H.K. Beyer, H.G. Karge, I.W. Mishin, J. Phys. Chem. 93 (1989) 3240.
[5] B. Sulikowski, J. Klinowski, J. Chem. Soc. Farad. Trans. 86 (1990) 199.
[6] G.W. Skeels, D.W. Breck, in: D.H. Olson, A. Bisio (Eds.), Proceedings of the 6th International Zeolite Conference, Butterworths, Guildford, 1984, p. 87.
[7] Z. Olejniczak, B. Sulikowski, A. Kubacka, M. Gąsior, Top. Catal. 11/12 (2000) 391.
[8] D.W. Breck, Zeolite Molecular Sieves, Wiley, New York, 1974.
[9] P.A. Vaughan, Acta Crystallogr. 21 (1966) 983.
[10] I.S. Kerr, Nature 210 (1966) 294.
[11] D. Seddon, J. Catal. 98 (1986) 1.
[12] R. Rachwalik, Z. Olejniczak, B. Sulikowski, Catal. Today 101 (2005) 147.
[13] P. Sarv, B. Wichterlová, J. Čejka, J. Phys. Chem. B 102 (1998) 1372.
[14] J. Datka, M. Kawałek, K. Góra-Marek, Appl. Catal. A 243 (2003) 293.
[15] D.P.B. Peixoto, S.M. Cabral de Menezes, M.I. Pais da Silva, Mater. Lett. 4451 (2003) 1.
[16] W.J. Taylor, D.W. Wagman, M.G. Williams, K.S. Pitzer, F.D. Rossini, J. Res. Natl. Bur. Stand. 37 (1946) 95.
[17] B. Sulikowski, R. Rachwalik, et al., in preparation.